

LIMUS: Exploration of Technological Prototypes for Location-Based Services in Museums *

Juan D. Gutiérrez, Fernando J. Aranda, Teodoro Aguilera and
Fernando J. Álvarez

*Department of Electrical Engineering, Electronics and Automation
Sensory Systems Research Group (<https://giss.unex.es/>)
University of Extremadura, Badajoz, Spain (06006)
andy@unex.es*

Abstract. This paper explores three technologies: acoustic, visible light, and Bluetooth Low Energy (BLE) to provide Location-Based Services (LBS) in museums or archaeological sites. Acoustic and visible light beacons have been specifically designed, whereas for BLE a commercial beacon has been chosen. Also, a mobile phone application has been developed which implements the identification algorithms for each proposed technology. Once the artwork has been identified, its information is displayed on the mobile phone screen. A set of experimental tests has been carried out in order to evaluate the performance of each technology. Results have shown a robust detection radius of 1.5 m around the acoustic and BLE beacons, while this radius decreases to 0.5 m for the visible light beacon. Results have also revealed the existence of some phenomena that worsen the detection quality in certain areas. This should be addressed in an evolved version of this work.

Keywords: Location-Based Services (LBS), Cell-ID, Acoustics, Bluetooth Low Energy (BLE), Visible Light, Museum.

1 Introduction

Location-Based Services (LBS) constitute the main reason that has fostered an intense research activity in the field of Local Positioning Systems (LPS). They can be generally defined as information services accessible with mobile devices through the mobile network and utilizing the ability to make use of the mobile device location [6]. In that sense, this work presents the development of a smartguide for archaeological sites in the Spanish region of Extremadura and the Portuguese region of the Alentejo (The LIMUS project [4]). This project aimed to design a common application for all visitors of a number of sites from the aforementioned regions, sites with very distinct characteristics that may require different tag identification technologies. Three of these technologies, namely acoustic, Bluetooth Low Energy (BLE), and visible light were finally selected to conduct a comparative analysis of performance. The results are presented in this work.

The paper is organized as follows. Section 2 details the characteristics and components of each prototype. Section 3 explains the transmitter and receiver architectures for each technology. Section 4 presents the main results obtained in the experiments that have been carried out. Finally, Section 5 highlights the most relevant conclusions drawn from this work.

* This work was supported in part by the European Commission through the Project LIMUS under Grant 0246-LIMUS-4-E, in part by the Spanish Government and the European Regional Development Fund (ERDF) through the Project MICROCEBUS-UEX under Grant RTI2018-095168-B-C54, and in part by the Regional Government of Extremadura and ERDF-ESF under Project GR18038.

2 Beacons Description

This section describes the beacons used, which are based on three different technologies: acoustic, BLE, and visible light. For each beacon, its appearance, dimensions, and components are described. For acoustic and visible light technologies, the beacons have been specifically designed to optimise the size, price, and quality of emissions. However, for BLE technology, a commercial beacon has been chosen, since this technology has long been used in mobile phones.

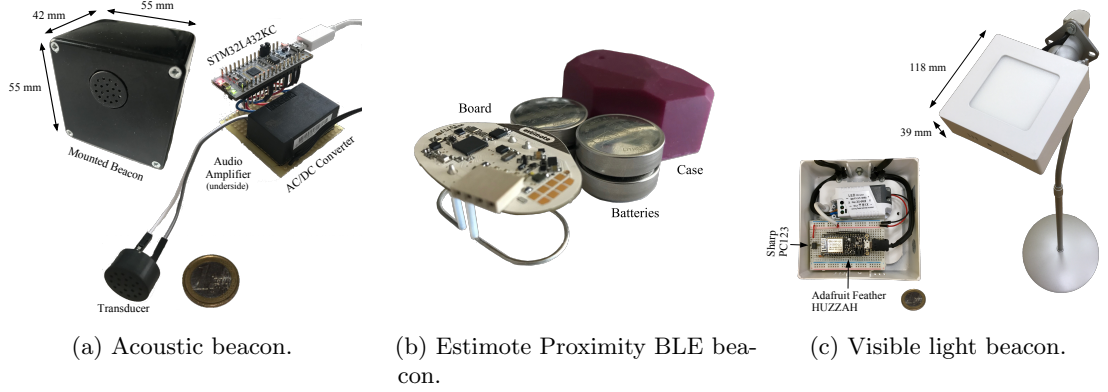


Fig. 1: Beacon description for each proposed technology.

Acoustic technology offers numerous advantages when it is used to implement systems that provide LBS. Among them, the narrow emission cone of the acoustic transducer makes it possible to discriminate between areas very close to each other. In addition, the acoustic waves will be confined in each museum room and detections from adjacent rooms will be avoided.

Fig. 1a shows on the right the inside of the beacon where an AC/DC converter, a NUCLEO-L432KC board and a KSSG1708 transducer can be seen. To the left of the figure can be seen the beacon mounted inside a plastic box of dimensions $55 \times 55 \times 42$ mm. This box has a perforation that allows the programming of the STM32L432KC module via its Micro-USB port. Furthermore, the beacon can be connected directly to the mains supply network without having to replace its batteries periodically.

Finally, this technology is suitable for the emission of robust signals against noise and the Doppler effect. This robustness makes it possible to implement modulations in long sequences generating 8 or even 16 bit encoding that can identify a large number of different exhibits.

The BLE beacons used for the LIMUS project are the Estimote BLE Proximity Beacons. As shown in Fig. 1b, these beacons have a low-power 32 bit and 64 MHz Central Processing Unit (CPU), a set of sensors (accelerometer, barometer, thermometer, magnetometer and photometer) and a Bluetooth antenna all over a circuit board. This device is powered by a set of batteries and wrapped in a plastic color case. Each beacon can broadcast multiple signals at the same time, using different emission powers and advertising periods. Estimote beacon's settings can be done via their smartphone application or cloud service. This beacon is shown in Fig. 1b.

Visible light beacon's final arrangement on a stand, as well as the beacon's insides, with its components identified, is shown in Fig. 1c. In particular, the beacon control and interruption circuit which modulates the light signal is implemented on a Feather Huzzah board manufactured by Adafruit. The combination of the CMOS cameras rolling shutter effect, the high frequency

LED luminaries modulation, and the human eye's inability to perceive them are the basis of this system [2]. Thus, it is possible to emit a luminous message without annoying people close to source.

3 Systems Operation

This section shows the beacons architecture. The transmitter operation for each technology is presented, as well as the particularities of their own receivers.

Fig. 2 shows the operating diagrams of both the transmitter and receiver modules for the acoustic technology. The transmitter module consists of an AC/DC converter in charge of supplying the STM32L432KC board. This board has a microcontroller STM32F103CBT6 that generates the digital signals. Subsequently, these signals pass through the board's digital-to-analog converter (DAC), to finally be sent to the amplifier in order to be synthesized using an acoustic transducer. The receiver module is implemented in an Xiaomi Mi 8 Android terminal. The phone acquires the acoustic signals through its embedded microphone. These signals are then processed by the phone's analog-to-digital converter (ADC). The resulting signal is first passed through a matched filter with a synchronization chirp (*initChirp*). The compressed pulse detection of this chirp indicates the beginning of the signal fragment where the information of the exhibit to be decoded is located. To decode this information, this signal fragment will be sent to two new filters. A first matched filter with the *upChirp* pattern determines the location of the compressed pulses corresponding to the chirps encoding the 1s, and a second matched filter now with the *downChirp* pattern determines the location of the compressed pulses identifying the 0s of the binary code. Then, in the decision module, the signals resulting from the matched filters are divided into sections of duration T_b (bit period). Both filtered signals are compared section by section, assigning the value 1 or 0 to the bit depending on whether the absolute maximum value for both filtered signals in the section in question corresponds to the pattern *upChirp* or *downChirp* respectively. Finally, an 8 bit binary code will be obtained which identifies the artwork in question. In addition, the use of frequencies in the audio's upper spectrum, together with the very low power emission that allows the chirp's pulse compression, makes the emission of these signals practically imperceptible to the users.

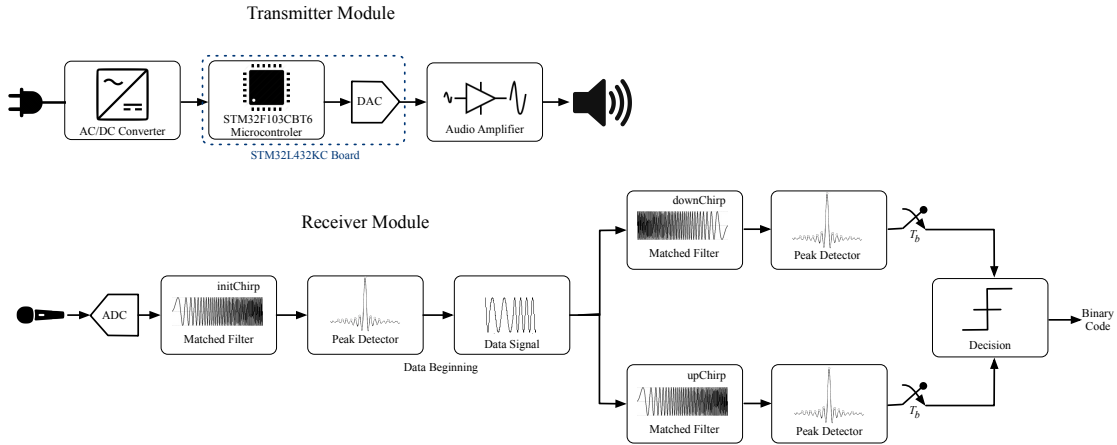


Fig. 2: Operating diagram of the transmitter and receiver acoustic modules.

The parameter used for positioning with BLE is the Received Signal Strength Indicator (RSSI). This value measures signal attenuation in a logarithmic scale and can be obtained from a smartphone device. RSSI decreases with the square of the distance from the source, but indoors multipath effect and emission frequency changes make measurements disperse and time variant [1]. The smartphone used as receiver performs a periodic scanning process, searching for other BLE devices in the surroundings. In each scanning, RSSI results are sorted from highest to lowest. The output code is the one associated with the first element of the list provided that its RSSI is above a threshold value, U_1 . This value is fixed to detect the code in the proximity of the beacon, otherwise the system can detect the code even at large distance inside the BLE maximum transmission range.

There could be situations when nearby beacons have high RSSI readings and all values are above the threshold U_1 . In order to avoid detections in these situations, the RSSI of the second element of the sorted list must be smaller than a second threshold, U_2 . Finally the whole process must be repeated three times to correctly identify the code and avoid false positive identifications. The whole process is shown in Fig. 3, where χ_{RSSI_i} is the output code of the system.

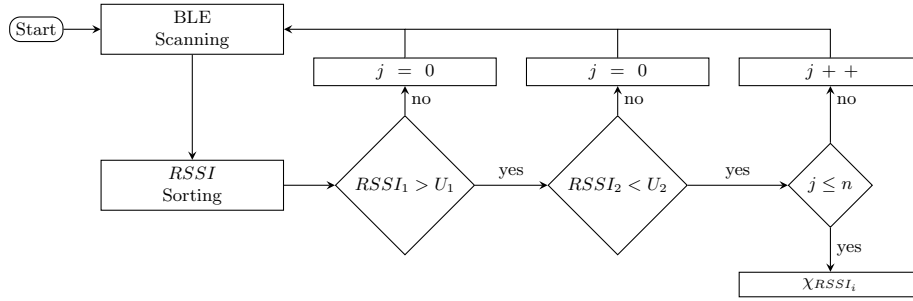


Fig. 3: BLE proposed code identification.

Fig. 4a shows the operating diagram of the visible light beacon transmitter module, while the block diagram that describes the acquisition and further signal processing is shown in Fig. 4b. The transmitter module needs two AC/DC converters, the first for the LED panel, the second for the Feather Huzzah development board, which is used to interrupt the power supply with the help of an optocoupler. The board is programmed to convert the message to a Manchester encoding via on-off keying (OOK). The LED panel turns off completely to transmit a 0 and lights up to transmit a 1, at an oscillation frequency of 5 kHz.

The Android app visible light detection module uses the rear camera of the terminal for the acquisition of the signal. First, the sensitivity of the camera is increased to the maximum, while its exposure time is reduced as much as possible. As a result, the luminous parts of the captured scene are more prominent than the rest, giving priority to luminaries. A single photograph is enough to carry out a complete decoding process. This process is repeated as many times per second as the capacity of the smartphone allows, twice in this work.

First, the acquired image is converted to gray scale, since only the intensity of the signal, not its chromatic components, are of interest. Next, the signal noise is reduced using a Gaussian smoothing function. Finally, a thresholding operation is performed, resulting in a black and white image. Otsu's algorithm [3] is applied to obtain the optimal threshold value. The second phase of processing begins with a reduction operation applied to the image columns, using the average of all the values. Otsu's thresholding is reapplied to the value vector obtained. The result of this

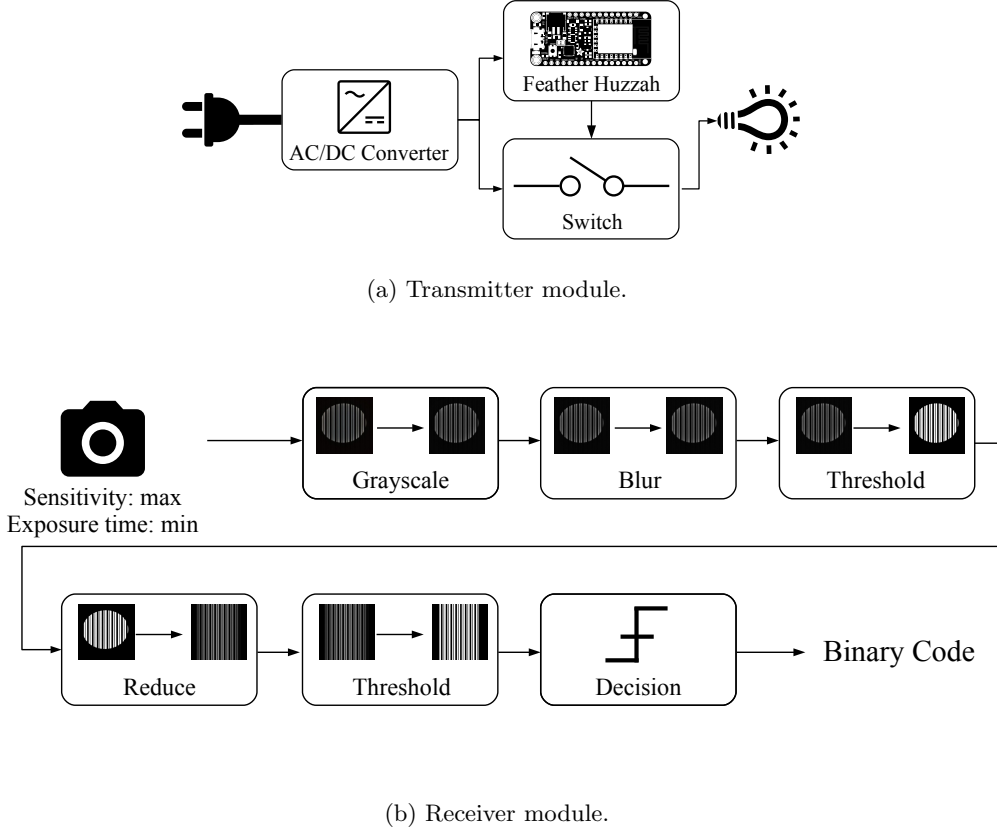


Fig. 4: Visible light beacon operating diagrams.

phase is a series of zeros and ones that can be processed to decode the message. The third and final signal processing phase looks for matches between the sequence of zeros and ones in the received message and the patterns. If said message is received three times consecutively, it is considered to be correct and sent as the output of the receiving module.

4 Experimental Results

In this section, a performance study of each technology will be carried out. To this end, the efficiency of these systems will be studied, evaluating the detection success in the surroundings of each type of beacon.

As depicted in Fig. 5a, both the beacon and the receiver (mobile phone) are mounted on a tripod. The beacon is placed at the origin of coordinates and the receiver is moved to the positions defined by a grid whose dimensions and spacing depends on the coverage area offered by each technology. For each test point, the mobile phone has taken 100 consecutive acquisitions of the beacon's identification signal, and the percentage of successful detections has been calculated.

The acoustic beacon was studied first. The emitting beacon was placed at 1.125 m height on a stand located at the coordinates origin of a grid with dimensions of $2.4 \times 2.4 \text{ m}^2$ and spacing of 0.4 m. On the other hand, the mobile phone was installed on an adjustable tripod, matching its

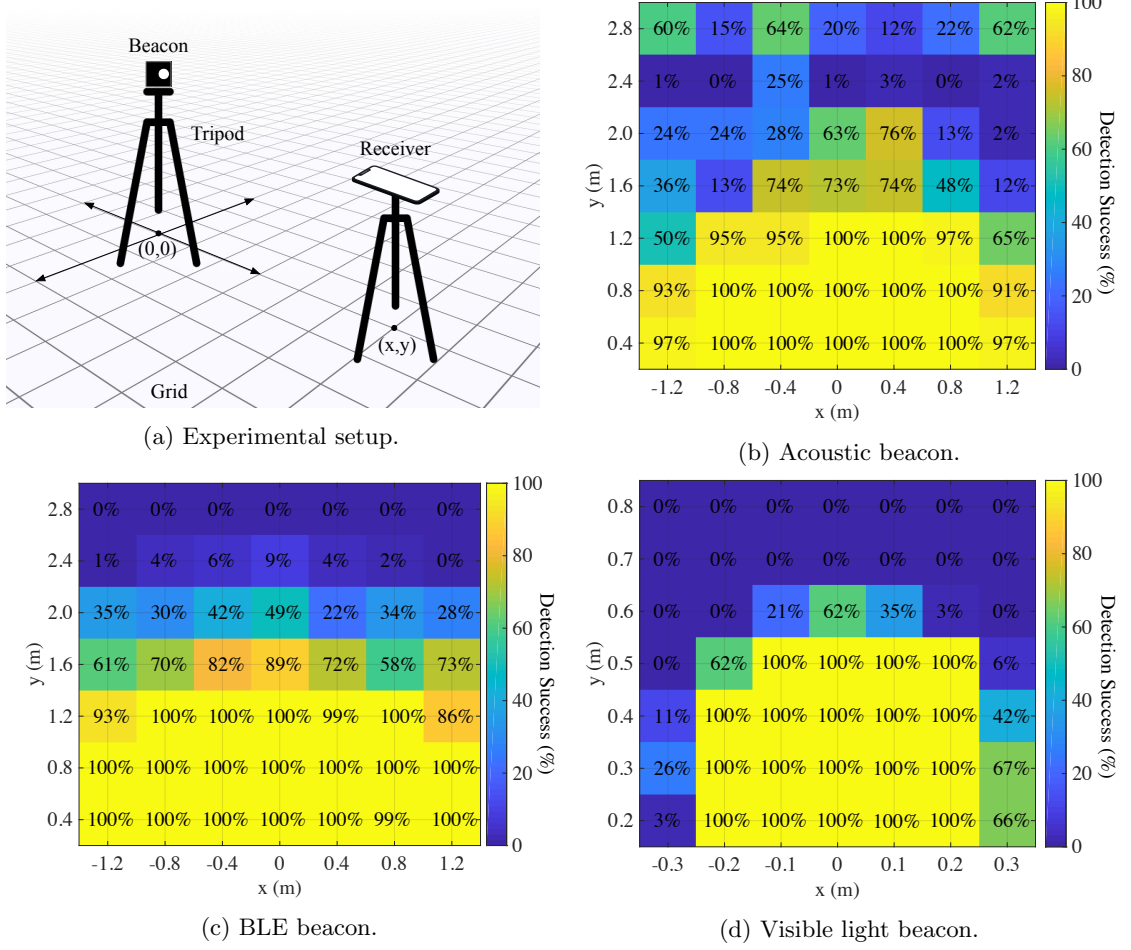


Fig. 5: Experimental setup (a) and results (b), (c), and (d).

microphone height with the one previously established for the acoustic emitter. In this way, both the transmitter and receiver acoustic axes are aligned. Therefore, a grid of $7 \times 7 = 49$ points was obtained with a separation of 0.4 m between each of them. The results are shown in Fig. 5b, where a robust detection ($> 90\%$) area of approximately 1.2 m radius semicircle around the acoustic beacon can be observed. Beyond this area it can be noticed how the detection success decreases due to the effect of several factors (combined or not) such as the distance signal attenuation, the relative transmitter/receiver orientation, and the multipath effect produced by walls, furniture, and floor. It is worth mentioning that the row at $y = 2.4$ m has a detection success practically null due to the multipath produced by the floor.

For the study of the BLE technology the same experimental setup used for the acoustic technology was employed. The beacon was placed at 1.175 m height on the same stand and the same 7×7 grid was used for measurements. The mobile phone was placed in an adjustable tripod, with no further considerations regarding its alignment since mobile and BLE beacon antenna have uniform polarization [5]. Fig. 5c shows a detection rate higher than 90% in an area of 1.2 m around the beacon. Beyond this, the detection rate decreases because the RSSI value

is below the U_1 threshold. Since consecutive RSSI measurements are very sparse, the change in the detection rate is not abrupt, with a small region featuring a detection rate around 50%. The threshold defines an area around the beacon where code detection is expected. Threshold increase or decrease changes the area with a high detection rate, thus it must be fixed beforehand according to the location and the minimum separation between exhibits.

A grid of 60×60 cm, with cells of 10×10 cm, was prepared for testing the visible light beacon performance. The light source was located 20 cm away from the middle of the grid. The center of the transmitter was located at 1 m height, as it was the camera optical axis. Both transmitter and receiver were parallel to each other. Given the differences in coverage between the two previous technologies and this one, using the same grid for the three experiments would have less accurate results for the case of visible light. There is a clear limit marked at a distance of about $y = 0.5$ m where the success rate decreases rapidly, as shown in Fig. 5d. For longer distances, detection is unfeasible due to the physical limitations imposed by the size of the emitting source, the camera resolution, and interference from other light sources present in the environment.

5 Conclusions

This work has explored different Location Based Services (LBS) technologies for mobile phones in museum environments. Concretely, acoustic technology, Bluetooth Low Energy (BLE), and visible light have been evaluated. Acoustic and visible light transmitter beacons have been specifically designed. Since BLE is a consolidated technology, an available commercial beacon has been chosen. Besides, the design and operation principle of each beacon has been explained. Also, the design of the mobile phone code detection algorithm for each technology has been described.

Moreover, an experimental study of detection robustness in the surroundings of each beacon has been carried out. This study shows that both the acoustic technology and BLE beacons have a robust detection radius of about 1.5 m around the beacon where the percentage of detections is above 90%. However, the visible light beacon detection radius is lower, around 0.5 m. According to the results, the three technologies have zones where the detection percentage decreases due to different factors that mask or deteriorate the signal. These issues should be addressed in later developments of this work.

References

1. Faragher, R., Harle, R.: Location fingerprinting with Bluetooth Low Energy beacons. *IEEE Journal on Selected Areas in Communications* **33**, 1–1 (11 2015). <https://doi.org/10.1109/JSAC.2015.2430281>
2. Gutiérrez, J.D., Álvarez, F.J., Aguilera, T., Paredes, J.A., Morera, J.: Visible Light Positioning for Smartphones Based on Biphase Mark Coding: A Proof of Concept. In: 2018 International Conference on Indoor Positioning and Indoor Navigation (IPIN) (2018)
3. Otsu, N.: A Threshold Selection Method from Gray-Level Histograms. *IEEE Transactions on Systems, Man, and Cybernetics* **9**(1), 62–66 (Jan 1979). <https://doi.org/10.1109/TSMC.1979.4310076>
4. Sensory Systems Research Group: Presentation of the Limus project, <https://giss.unex.es/2019/03/21/presentation-of-the-limus-project/>
5. The Bluetooth Special Interest Group: Kirkland, WA, USA: Specification of the Bluetooth System, Covered Core Package, Version: 4.0
6. Virrantaus, K., Markkula, J., Garmash, A., Terziyan, Y.: Developing GIS-supported location- based services. In: First International Workshop on Web Geographical Information Systems (WGIS 2001). p. 423–432. Kyoto, Japan (2001)